An isolation enhanced PCA method with expert-based multivariate decoupling for sensor FDD in air-conditioning systems

Article *in* Applied Thermal Engineering · March 2009

DOI: 10.1016/j.applthermaleng.2008.03.046

CITATIONS
43

READS
107

4 authors:

Linda F. Xiao
The Hong Kong Polytechnic University
99 PUBLICATIONS **1,820** CITATIONS
SEE PROFILE

Shengwei Wang
The Hong Kong Polytechnic University
263 PUBLICATIONS **5,539** CITATIONS
SEE PROFILE

Xinhua Xu
53 PUBLICATIONS **1,021** CITATIONS
SEE PROFILE

Gaoming Ge
University of Saskatchewan
39 PUBLICATIONS **706** CITATIONS
SEE PROFILE

Applied Thermal Engineering 29 (2009) 712–722

Contents lists available at ScienceDirect

Applied Thermal Engineering

journal homepage: www.elsevier.com/locate/apthermeng

An isolation enhanced PCA method with expert-based multivariate decoupling for sensor FDD in air-conditioning systems

Fu Xiao [a,*], Shengwei Wang [a], Xinhua Xu [b], Gaoming Ge [a]

[a] Department of Building Services Engineering, The Hong Kong Polytechnic University, Kowloon, Hong Kong
[b] Department of Building Environment and Services Engineering, School of Environmental Science & Engineering, Huazhong University of Science & Technology, Wuhan, China

ARTICLE INFO

Article history:
Received 10 December 2007
Accepted 25 March 2008
Available online 7 April 2008

Keywords:
Principle component analysis
Fault detection and diagnosis
Sensor fault
Multivariate decoupling
Air-handling process

ABSTRACT

Principal component analysis (PCA) has been found to be powerful in detecting sensor faults in multivariate processes, but it is inefficient in isolating faults due to its pure data-driven nature, especially when dealing with processes with strongly coupled multiple variables, such as the air-handling processes in typical variable air volume air conditioning systems. This paper presents an expert-based multivariate decoupling method to enhance the capability of the PCA-based method in fault diagnosis by taking advantage of expert knowledge about the process concerned. The decoupling method develops unique fault patterns of typical sensor faults by analyzing the physical cause-effect relations among variables. Through comparing fault symptoms reflected by the residual vectors of the PCA models with fault patterns, a sensor fault can be successfully isolated. The isolation enhanced PCA method is implemented and validated in a typical air-handling process. The test results show that the joint approach to enhance the fault isolation ability of the PCA-based fault detection and diagnosis method is effective. The robustness of the PCA-based sensor FDD method against component faults is also proved to be improved because the fault symptoms of sensor faults are unique.

1. Introduction

Principal component analysis (PCA) [1,2] has shown its powerful ability in detecting faults in various industrial and engineering processes, including chemical processes [3–6], semiconductor processing [7], machining process [8], waste water treatment [9], nuclear power system [10], air-conditioning processes [11,12], building central chilling system [13], etc. Most processes are well equipped with sensors to realize automatic monitoring and control. The sensor measurements provide redundant information for sensor fault detection and diagnosis (FDD) because they are highly correlated or strongly coupled due to basic principles governing the process, such as energy and mass conservations and feedback control loops. Sensor faults may disturb the normal correlations among sensor measurements. Statistic PCA models, which are built using historical data under normal operating condition, can be used to monitor correlations among sensor measurements in a dimension-reduced subspace. Statistics are used as fault indexes, which will increase significantly to abnormal level if sensor faults occur. One typical monitoring statistic is the Q-statistic or squared predictive error (SPE). Once a fault is detected by the Q-statistic, the Q-contribution plot is often used to diagnose this fault. The sensor that has a major contribution to the Q-statistics is considered to be most probably faulty.

Although fault detection can be performed efficiently using the PCA-based FDD method, approaches for fault diagnosis using PCA are less well developed. Most of modern processes, such as the air-handling process, have the features of strongly coupled multivariables and multi-control loops. While all the control loops are working together, they interfere with and influence each other, which causes the control unstable and even totally out of control. At the same time, due to the couplings among multiple control loops, fault in one control loop may propagate to other loops, which causes the faulty symptoms very complicated and consequently it is not easy to find out the origin of the fault during operation and maintenance. As a widely used fault isolation approach in the PCA-based FDD method, the Q-contribution plot is inefficient in isolating sensor faults, especially when dealing with sensor faults whose effects may propagate to other parts of the process and cause symptoms there. It is important to improve the fault isolation ability of the PCA-based FDD method.

The weakness of PCA in isolating faults is inevitable due to its pure data-driven nature, which considers the process concerned as a black box and less knowledge about it is used. Some approaches have been developed to improve the isolation ability of the PCA-based FDD method. Gertler et al. [14] introduced a valuable analytical redundancy (AR) concept to the PCA method

* Corresponding author. Tel.: +852 2766 4194; fax: +852 2774 6146.
E-mail address: befx@polyu.edu.hk (F. Xiao).

1359-4311/$ - see front matter © 2008 Elsevier Ltd. All rights reserved.
doi:10.1016/j.applthermaleng.2008.03.046

Nomenclature

A	training matrix of the heat balance PCA model
B	training matrix of the pressure-flow balance PCA model
C	control signal
Cov	covariance matrix of X
C_x	projection matrix
e	residual
h	humidity (kg/kg)
M	flow rate (kg/s)
P	pressure (Pa)
Q_α	threshold of Q-statistic
R	covariance matrix
T	temperature (°C)
X	variable matrix under normal operation conditions ($X \in R^{n\times m}$), n samples of m variables
x	vectors of variables ($x \in \Re^m$)
L	loading vectors

Greek symbols

σ	standard variance
Ψ	diagonal matrix

Subscripts and superscripts

coil	cooling coil
exh	exhaust air
fanr	return air fan
fans	supply air fan
fre	fresh air
new	new samples
rtn	return air
sup	supply air
val	valve
w	chilled water
$\wedge$	estimated output
–	normalized matrix

by utilizing the equivalence between PCA and parity relations. Structure residuals were so designed that each residual was sensitive to a particular subset of faults. With a suitable combination of residual structures, each fault triggered a characteristic response, called its fault code. The method tried to isolate faults by mathematically decoupling variables. Structure residuals obtained by PCA had the same isolation ability as AR residuals. However, it is not easy to design the structure matrix. Which residual is sensitive to a particular fault is mathematically determined. It may cause ambiguity if a fault propagates to other variables. The computation intensive problem also limited its practical application.

Vedam and Venkatasubramanian [15] adopted signed digraph, which is a qualitative model of the causal interactions between different variables in a process, to interpret the Q-contributions of each variable in a PCA model. They considered that variables giving larger contributions to the Q-statistic represented the propagation route of the sensor fault. By comparing the propagation symptom with the real propagation routes, which were obtained by analyzing the signed directed graph (SDG) of the process, the faulty sensor can be isolated. The SDG-based analysis fully took advantage of the knowledge about the process. However, the method to choose the thresholds of the Q-contributions is somehow subjective.

There are still a few other methods which require either additional data on past faults or fault database, such as the method proposed by Yoon and MacGregor [16]. It is difficult to get complete fault database due to faults cannot be introduced to a real process. Both the fault isolation method proposed by Wise and Ricker [17], which was based on reconstructing each variable using the PCA models, and the method based on a sensor validity index (SVI) proposed by Dunia and Qin [4] met great challenge while dealing with faults whose effects may propagate to the other variables. The improved PCA with joint angle analysis (JAA) method proposed by Du and Jin [18,19] can isolate the fault propagate in the local loop, but it is difficult to identify the fault source when the fault propagate among multi-loops. In summary, difficulties mainly come from the requirements on the knowledge about fault propagation. It is not easy to overcome those difficulties in application.

This study develops an approach that provides more reliable fault isolation results while dealing with sensor faults and component faults by combining the Q-contribution plot with expert-based multivariate decoupling. Physical expert knowledge about the process is planted into the data-driven PCA method. The isolation enhanced PCA method is implemented and validated in a typical air-handling process.

2. Typical air-handling process and multivariate coupling problems

The air-handling processes in VAV air-conditioning systems are complex control processes, which have the features of strongly coupled multi-variables and multi-control loops. A typical air-handling unit (AHU) with typical monitoring and control instrumentation is considered in this study as shown in Fig. 1. To achieve acceptable indoor air quality and minimize energy consumption, essential control loops include the supply air temperature control loop, the supply air static pressure control loop, the room temperature control loop, the room humidity control loop, the return fan control loop and the interlocked control loop of the dampers of fresh air, return air and exhaust air. PID controllers are usually adopted in these local control loops. Besides, typical but advanced control strategies are adopted to provide adequate outdoor air ventilation, and to minimize energy use, such as economizer and demand controlled ventilation [20,21]. The couplings or interactions among these control loops and control strategies make the fault isolation very difficult, because the fault may be hidden due to the feedback of the symptoms or the fault propagates among multiple control loops. Decoupling multiple variables can not only improve the real-time control performances in VAV systems, but also benefit their lifecycle performances.

The sensor instrumentation in Fig. 1 is also typical for implementing the control strategies. The sensor instrumentation includes temperature sensors of the fresh air, return air and supply air, flow rate sensors of the fresh air, return air and supply air, humidity sensors of the return air and fresh air and the static pressure sensor of supply air. Totally, nine sensors are employed. These sensors are important elements in an air-handling process to realize automatic monitoring and control. Their faults may misrepresent the operating conditions, mislead the system controls and consequently cause energy waste and indoor environment quality deterioration.

In VAV systems, while multiple control variables are controlled simultaneously and all the control loops are working together, they interfere with and influence each other, which may deteriorate the reliability and stability of VAV systems [22]. For examples, the

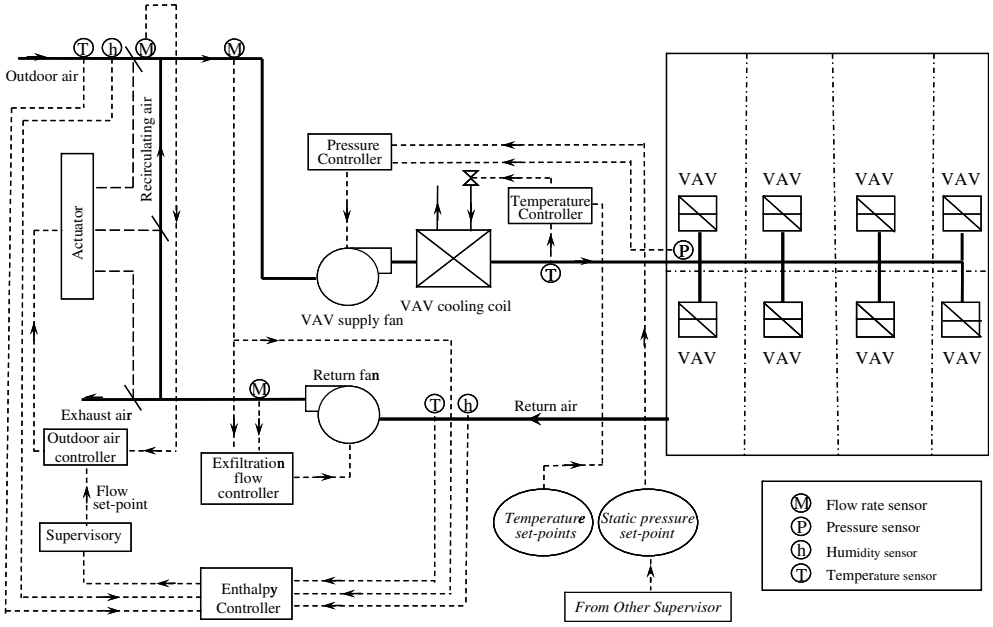

Fig. 1. Schematic of VAV system and measurement instrumentation.

change of the chilled water flow rate influences the supply air temperature, while this change will influence the supply air flow rate to maintain indoor thermal environment. The change of the supply air flow rate influences the indoor air temperature, while this change also result in the change of the air flow rate through the cooling coil, and consequently the supply air temperature is also influenced.

Problems caused by couplings among multi-variables and multi-control loops widely exist in modern automatic processes. Many efforts have been taken to decouple multi-variables and multi-control loops in not only air-conditioning industry [23,24] but also many other fields, such as chemical processes [25], paper industry [26], satellite launcher [27] etc. A neural network with proportional, integral and derivative (PID) neurons was used to decouple the control of strongly coupled multivariable systems [28]. Multivariable cascade control was used to decouple the control of indoor temperature and relative humidity [24]. Wang and Wang [23] developed a feedforward compensation decoupling method combined with genetic algorithm for eliminating the couplings among multiple control loops in VAV system. In most previous research, pure mathematic methods were used, which took little advantage of knowledge about the process concerned and suffered from practically unaffordable computation load. Considering existing rich knowledge about VAV systems nowadays, this study aims at developing an isolation enhanced-PCA method with expert-based multivariate decoupling for sensor FDD in VAV systems. A typical VAV air-conditioning system simulator, which is developed by Wang on the platform of TRNSYS [20], is used in the test and validation in this study.

3. PCA-based sensor FDD for VAV air conditioning system

3.1. Outline of PCA method in FDD application

PCA is a popular multivariate statistical analysis method. Two most important functions of PCA are dimension reduction and orthogonal decomposition. Variables in a modern engineering process are usually multi-dimensional and correlated. The correlations among process variables can be represented by a smaller number of variables because of the redundancy of the process variables.

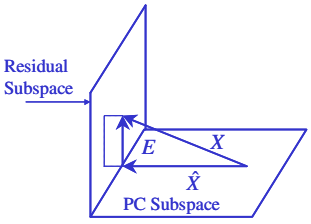

Fig. 2. Decomposition of measurement space.

The use of PCA to build low dimensional models for monitoring the correlations is well developed. Measurement space (X), constructed by measurements of correlated process variables, can be decomposed into two orthogonal subspaces using the PCA method, i.e., the residual subspace (E) and the principle component (PC) subspace ($\widehat{X}$) as shown in Fig. 2 and Eq. (1). X can be mathematically defined using a matrix of the order of n rows (samples) and m columns (process variables). This matrix also constructs a PCA model.

$$X = \widehat{X} + E \tag{1}$$

The PC subspace contains the major normal variations of the correlations. The direction of the PC subspace is defined by the loading vectors (L), which are parts of the eigenvectors of the covariance matrix (Cov) of X. In practice, Cov is usually estimated from samples of variables under normal condition as shown in Eq. (2).

$$Cov = X^{\mathrm{T}}X/(n-1) \tag{2}$$

Usually, Cov has m eigenvectors. In the application of PCA, only those eigenvectors, L ($L \in \Re^{m\times k}, k < m$), which are associated with the first k largest eigenvalues, are retained in the PCA models, because they represent the direction of most variance of a process. Therefore, the original m-dimensional measurement space can be represented by the k-dimensional PC subspace. There is no optimal criterion for choosing k. Edward [1] suggested about ten commonly used criteria, such as the proportion of trace explained, individual residual variances, the screen test, and cross-validation.

While a new sample ($x_{new} \in R^m$) is monitored, it can be decomposed into two parts as shown in Eq. (3). $\hat{x}_{new}$ is the projection on the PC subspace containing the main variations of the process correlations, and e is the projection on the residual subspace known as residual vector.

$$x_{new} = \hat{x}_{new} + e \tag{3}$$

The projection matrix (C_x) of projecting x_{new} on the PC subspace is calculated using Eq. (4), given that the loading vectors L are orthonormal. $\hat{x}_{new}$ is calculated using Eq. (5), and the residual vector, i.e., $e \in R^m$ is calculated using Eq. (6).

$$C_x = L(L^{\mathrm{T}}L)^{-1}L^{\mathrm{T}} = LL^{\mathrm{T}} \tag{4}$$

$$\hat{x}_{new} = C_x x_{new} = LL^{\mathrm{T}}x_{new} \tag{5}$$

$$e = x_{new} - \hat{x}_{new} = (I - LL^{\mathrm{T}})x_{new} \tag{6}$$

In FDD applications, the squared sum of the residual, namely the Q-statistic or squared prediction error (SPE) calculated using Eq. (7), is used as an index of faulty conditions.

$$Q\text{-statistic} = \mathrm{SPE} = \|e\|^2 = \|(I - LL^{\mathrm{T}})x_{new}\|^2 \leqslant Q_\alpha \tag{7}$$

where Q_α denotes a statistical threshold for the Q-statistic [1]. When no fault exits, the Q-statistic or SPE, which is less than Q_α, represents the normal dynamics and measurement noises, etc., of the process that cannot be captured by the PCA model. On the other hand, when a sensor fault occurs, the correlations among the measurements of the variables will be destroyed, and a higher value of the Q-statistic is detected.

Once a fault is detected using the Q-statistic, the Q-contribution plot can be used to diagnose the fault. The contributions of the individual variables to the Q-statistics are compared, and the variable making the largest contributions to the Q-statistics is most probably faulty.

3.2. Application of PCA method in VAV system sensor FDD

The PCA method has been successfully applied to detection and diagnosis of AHU sensor faults [11]. Two PCA models, the heat balance model and the pressure-flow balance model are built to make variables in individual model more closely correlated, and to facilitate fault diagnosis because different models are sensitive to different sensor faults. Some control signals are also included in the PCA models to make correlations closer. The PCA model based on the heat balance involved nine variables: M_{fre}, M_{sup}, M_{rtn}, T_{fre}, T_{sup}, T_{rtn}, h_{fre}, h_{rtn}, and $C_{val,\ w}$, which constructed a nine-dimensional measurement space. This model could detect faults in eight sensors in the VAV system, except for the pressure sensor. The PCA model based on the pressure-flow balance of the process involved six measured variables: M_{fre}, M_{sup}, M_{rtn}, P_{sup}, C_{fans} and C_{fanr}, where C_{fans} and C_{fanr} were the supply and return fan control signals, respectively, which constructed a six-dimensional measurement space. All these measurements are typically available in building automation systems.

$$A = \begin{bmatrix} M^1_{fre} & M^1_{sup} & M^1_{rtn} & T^1_{fre} & T^1_{sup} & T^1_{rtn} & h^1_{fre} & h^1_{rtn} & T^1_{w,sup} & C^1_{w,val} \\ M^2_{fre} & M^2_{sup} & M^2_{rtn} & T^2_{fre} & T^2_{sup} & T^2_{rtn} & h^2_{fre} & h^2_{rtn} & T^2_{w,sup} & C^2_{w,val} \\ . & . & . & . & . & . & . & . & . & . \\ M^n_{fre} & M^n_{sup} & M^n_{rtn} & T^n_{fre} & T^n_{sup} & T^n_{rtn} & h^n_{fre} & h^n_{rtn} & T^n_{w,sup} & C^n_{w,val} \end{bmatrix}_{80\times 9}$$

$$B = \begin{bmatrix} M^1_{fre} & M^1_{sup} & M^1_{rtn} & P^1_{sup} & C^1_{fans} & C^1_{fanr} \\ M^2_{fre} & M^2_{sup} & M^2_{rtn} & P^2_{sup} & C^2_{fans} & C^2_{fanr} \\ . & . & . & . & . & . \\ M^n_{fre} & M^n_{sup} & M^n_{rtn} & P^n_{sup} & C^n_{fans} & C^n_{fanr} \end{bmatrix}_{80\times 6}$$

In order to obtain the loading vectors (L) and the threshold of the Q-statistic, two training matrixes were constructed from 80 samples of normal data. Matrix A was used to train the heat balance model and matrix B was used to train the pressure-flow balance model. Since the variables were of different units in the VAV system, the data in each column were normalized to zero mean and unit variance.

$$M_a = \frac{1}{n}A^{\mathrm{T}}\mathrm{I}_n \tag{8}$$

$$\sigma_{ai} = \sqrt{\frac{1}{n-1}\sum_{j=1}^{n}(A_{j,i} - M_{ai})^2} \tag{9}$$

$$\overline{A} = (A - I_n M_a^{\mathrm{T}})\Psi^{-1}_{m\times m} \tag{10}$$

$$R_a = \frac{1}{n-1}\overline{A}^{\mathrm{T}}\overline{A} \tag{11}$$

Eqs. (8)–(11) demonstrate how to normalize the training matrix and calculate the covariance matrix of the training matrix A. Eq. (8) calculates the mean vector ($M_a \in \Re^{1\times m}$, here m = 9 for A) of matrix A, in which $\mathrm{I}_n = [1, 1, \ldots 1]^{\mathrm{T}} \in \Re^n$. Eq. (9) calculates the standard variance of the ith column of A, corresponding to the ith variables, where M_{ai} is the mean of the ith column of A. Matrix A is normalized to zero mean and unit variance as shown in Eq. (10), where $\Psi_{m\times m} = \mathrm{diag}(\sigma_{a1} \quad \sigma_{a2} \quad \cdots \quad \sigma_{am}) \in \Re^{m\times m}$ is a diagonal matrix whose ith diagonal element is the standard variance of the ith variables in A. The covariance matrix R_a is calculated according to Eq. (11).

The screen test has been used to determine the optimal number of the principle components of the PCA model [11]. It was found that the nine-dimensional heat balance measurement space can be reduced to a four-dimensional space, and the six-dimensional pressure-flow balance measurement space can be reduced to a two-dimensional space. The loading vectors (L) can be calculated from R_a using the iteration method [29]. The threshold of the Q-statistic can be calculated using the method proposed by Edward [1]. The thresholds were 2.0449 for the heat balance model and 0.1806 for the pressure-flow balance model.

While new samples, i.e., $x_{new} \in R^{n1\times m}$ ($n1$ is the number of new samples), were monitored, they were firstly normalized using the mean vector and the standard variance vector as shown in Eq. (12).

$$\bar{x}_{new} = (x_{new} - I_{n1} \times M_a)\Psi^{-1}_{n1\times m} \tag{12}$$

where I_{n1} and $\Psi_{n1\times m}$ have the same definitions as above except for different number of samples. The residual vector is calculated as Eq. (6) where L is the loading vector of the principal components, and the Q-statistics of new samples are calculated as Eq. (7).

The Q-statistics of new samples are compared with the threshold. Faults are detected by abnormally larger Q-statistics, and then diagnosed using the Q-contribution plot.

3.3. Test results and limitations of the PCA-based FDD method

Both simulation tests and tests using sitedata from an existing building were conducted to validate the PCA-based sensor FDD method for AHU [11]. Here, some test results are chosen to illustrate the performance of the PCA-based FDD method in detecting and diagnosing AHU sensor faults. Biases were introduced to all nine sensors in the air-handling process. Only one sensor was faulty in each of test cases. The results of the fault detection of sensor faults are shown in Fig. 3.

Fig. 3 shows that the heat balance PCA model successfully detected the sensor faults of the return air humidity, fresh air flow rate, supply air temperature, return air flow rate, fresh air temperature, fresh air humidity and return air temperature because their Q-statistics increased significantly and exceeded the threshold once faults occurred. However, the fault of the supply air pressure sensor, which occurred at 1:20PM, was not detected. This is because that the supply air static pressure sensor fault do not disturb

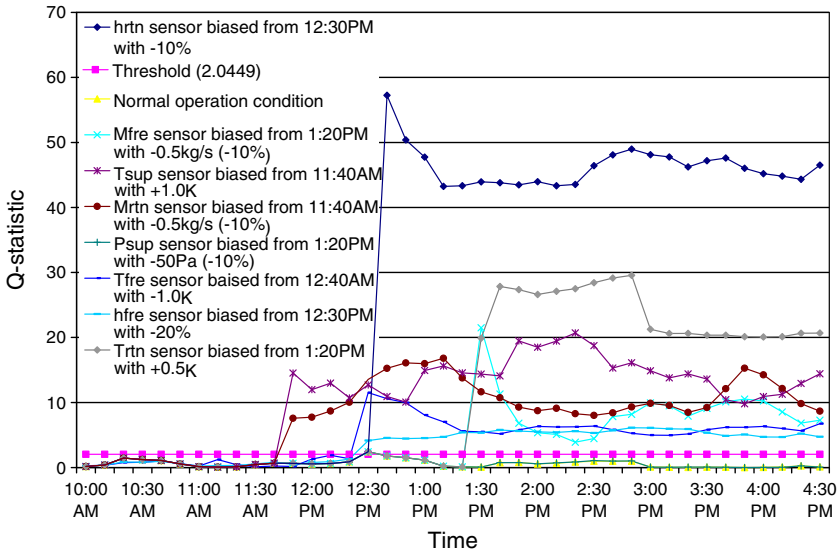

Fig. 3. Q-statistic plot of simulation tests (single sensor fault in each test case) – sensor faults detected using the heat balance model.

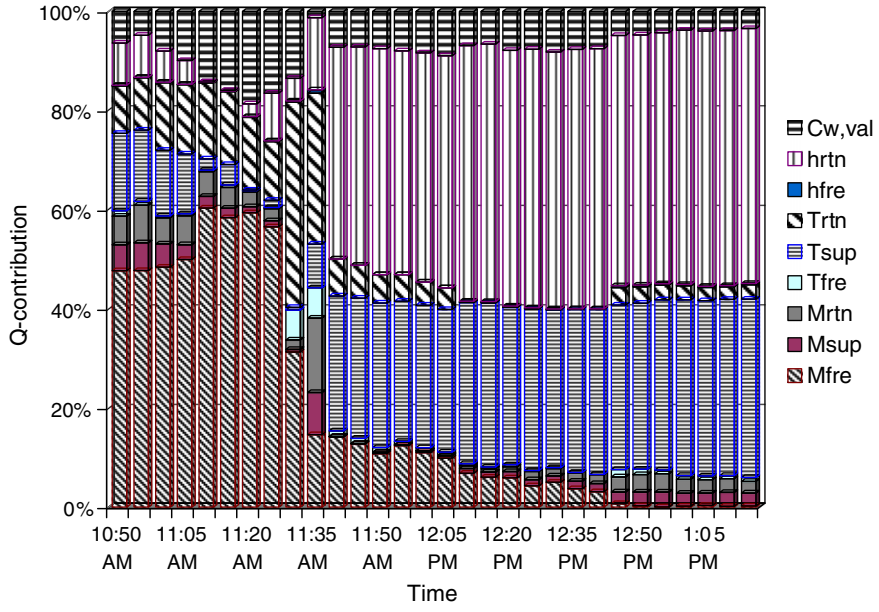

Fig. 4. Q-contribution plot of the heat balance PCA model. When T_{sup} sensor was biased with +1.0 K after 11:40 AM.

the heat balance couplings of the air-handling process, therefore the heat balance PCA model is insensitive to this kind of fault.

The use of the pressure-flow PCA balance model made the static pressure sensor faults detectable, as it was affected to pressure sensor faults. Test results showed that the faults in the fresh air, return air, and supply air flow sensors, and in the supply air pressure sensor were detected by the pressure-flow balance PCA model immediately after they occurred. However, the pressure-flow balance PCA model was not capable of detecting faults in the temperature and humidity sensors. This is because temperature and humidity sensor faults do not affect the pressure-flow balance couplings in the air-handling process.

The sensor fault test results show single PCA model is insufficient in detecting the faults of all sensors in the VAV system. It is necessary to use multiple PCA models in parallel and to make use of as many correlations as available among the measured variables. At the same time, the use of multiple models also provides great benefits in diagnosing fault sources. For example, if the heat model does not detect any abnormality (i.e., the Q-statistic generated by the measurements do not exceed the threshold of the heat balance model), but the pressure-flow balance model detects abnormality, the supply air pressure sensor is very likely faulty.

Once a fault was detected, it must be isolated for further maintenance. The Q-contribution plot has been used to diagnose faults. Test results showed that the faults of fresh air temperature, fresh air humidity and return air temperature sensors could be successfully isolated using the Q-contribution plot. However, the sensor faults of the supply air flow rate, supply air temperature, return air flow rate, supply air static pressure and the return air humidity could not be correctly isolated using the Q-contribution plot alone, because both the faulty measurements and measurements of the affected variables gave large contribution to the whole variance of the process, i.e., the Q-statistics. Fig. 4 shows the fault diagnosis result of the supply air temperature sensor using the Q-contribution

plot of the heat balance PCA model. The temperature sensor fault could not be diagnosed correctly because the return air humidity contributed most to the Q-statistics. It is because the return air humidity was affected by such a fault due to the coupling between the supply air temperature and the return air humidity (or between the supply air temperature control loop and the room air temperature control loop). Therefore, decoupling multiple variables in multiple control loops is important for diagnosing the sensor faults of VAV system, as well as the robust automatic control of VAV systems.

4. Isolation-enhanced PCA method with expert-based multivariate decoupling

The basic idea to improve the fault isolation ability of the PCA-based FDD method is to explore and make use of new fault symptoms besides the Q-contributions from the PCA-based FDD results. It was found in this study that the residual vectors, e in Eq. (6), could also reflect some faulty symptoms. The elements (e_i) represent the unmodeled variations of corresponding variables. The elements of the residual vector have two possible signs, positive and negative, which represent two changing directions, increase and decrease. Under normal conditions, the elements of e fluctuate around zero, but their squared sum, i.e., the Q-statistic, is under its statistical threshold with certain confidence level. The elements of e are seldom equal to zero due to process dynamics, measurement noises and other disturbances. In the use of the PCA method, each variable has a statistical expectation in the PCA model, defined by the historical data in matrix X. The residual vector indicates the discrepancies of the new samples to its statistical expectations. If the measurement of the *ith* variable is larger than its statistical expectation, the ith element of the residual vector e is positive. If the measurement of the ith variable is smaller than its statistical expectation, the ith element of the residual vector e is negative. The absolute values of the positive and negative elements represent the magnitudes of the unmodeled variances of the corresponding variables. By interpreting signs of the residual vector e, the changing directions of measured variables can be determined, which can be used as fault symptoms. On the other hand, although the changing magnitudes of the variables affected by some sensor faults are always difficult to be quantified in practice, the changing directions of the affected variables, namely fault patterns in this study, are certain and can be deduced from coupling characteristics. By comparing the fault symptoms reflected by the residual vectors and the fault patterns, the complex sensor faults can be isolated.

$$e_A = \begin{bmatrix} e_{M_{\mathrm{fre}}} & e_{M_{\mathrm{sup}}} & e_{M_{\mathrm{rtn}}} & e_{T_{\mathrm{fre}}} & e_{T_{\mathrm{sup}}} & e_{T_{\mathrm{rtn}}} & e_{h_{\mathrm{fre}}} & e_{h_{\mathrm{rtn}}} & e_{\mathrm{val,w}} \end{bmatrix}^{\mathrm{T}} \quad (13)$$

$$e_B = \begin{bmatrix} e_{M_{\mathrm{fre}}} & e_{M_{\mathrm{sup}}} & e_{M_{\mathrm{rtn}}} & e_{P_{\mathrm{sup}}} & e_{\mathrm{fans}} & e_{\mathrm{fanr}} \end{bmatrix}^{\mathrm{T}} \quad (14)$$

According to the PCA models built from Matrix A and B, the residual vectors obtained from the PCA models are shown as Eqs. (13) and (14). Fault symptoms can be obtained by interpreting signs of the residual elements. An approach based on multivariate decoupling is developed in this study to establish fault patterns as described below.

4.1. Expert-based multivariate decoupling

The expert-based multivariate decoupling method is developed from the rich knowledge and understandings of VAV systems, which utilizes the causal-effect interactions between different variables in VAV control process. When a sensor fault occurs, measurements of the sensor will be affected. At the same time, the fault very likely causes values of other variables to increase or decrease. In order to isolate the faulty sensor, fault patterns need to be established in advance. By matching the fault symptoms and fault patterns, the faulty sensor can be successfully isolated. Expert-based multivariate decoupling analysis developed in this study is, in fact, an effective tool to present and analyze the qualitative cause-effect relations. The method to set up fault patterns based on expert-based multivariate decoupling will be explained using the PID feedback control loop for controlling the supply fan speed to maintain the supply air static pressure at its setpoint as an example.

The physical causal-effect couplings in the static pressure control process (as shown in Fig. 5) are illustrated as an example here. The three variables involved in this control process are the static pressure, the control signal of the supply fan and the supply air flow rate which is affected by the control process due to the characteristic of the process. Assuming that the measurement of the static pressure increases, the control signal will decrease due to the feedback control. Therefore, their cause-effect relationship is negative. The decrease of the control signal of the supply fan will result in the decrease of the supply air pressure and supply air flow rate. Therefore, the cause-effect relations are positive.

If using a PCA model to represent the correlation among the pressure, control signal of fan and flow rate, signs of the elements in the residual vectors will reflect fault symptoms when a sensor fault occurs according to the above analysis. Assuming the static pressure sensor has a negative bias; its measurement will decrease and have a negative bias compared with the real pressure. Due to the feedback control, the control signal of the fan will increase, and consequently have a positive residual. The air flow rate will also increase according to the physical characteristic of the process, and consequently have a positive residual. Therefore, the fault patterns of the static pressure sensor faults can be described as shown in Table 1.

The fault patterns indicated in Table 1 can be described in details. If the static pressure sensor is negatively biased, its residual in the PCA model will be negative, the residual of the control signal will be positive and the residual of the flow rate will be positive too. Therefore, the residuals of the pressure, control signal of the fan and flow rate in the PCA model may have the signs as '−', '+', '+'. On the contrary, if the static pressure sensor is positive biased, its residual in the PCA model will be positive, the residual of the control signal will be negative and the residual of the flow rate will be negative as well. Therefore, the residuals of the pressure, fan control signal and flow rate in the PCA model may have the signs as '+', '−', '−'.

Comparing the fault symptoms reflected by the residual vector of the PCA model and the established fault patterns, the fault can be isolated successfully.

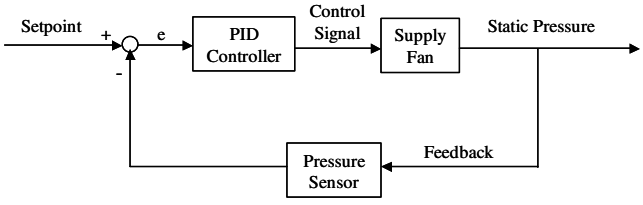

Fig. 5. Schematic of the static pressure PID feedback control loop.

Table 1
Fault patterns describing cause-effect relations in the PID feedback control loop

Sensor fault	Affected variable		
	Static pressure (P_{sup})	Control signal of fan (C_{fan})	Flow rate (M_{sup})
$P_{\mathrm{sup}}(-)$	−	+	+
$P_{\mathrm{sup}}(+)$	+	−	−

4.2. Development of fault patterns of a typical air-handling process

Experiences show that accurate mathematic model describing correlations among variables in a VAV system is inefficient in improving fault isolation ability. Fortunately, some well-known qualitative relations do help in setting up a qualitative model. These relations may remain unchanged even operation conditions change. In order to find out the propagation routes of a sensor fault, the algorithm of describing cause-effect relations between variables based on expert rules are adopted in this study.

There is no need to consider those sensors that do not participate in any feedback control loop and optimal control strategies because their faults may not affect other measurements, and consequently their faults can be diagnosed using the Q-contribution plot alone. The humidity and temperature sensors of the fresh air and the return air (four sensors in total) belong to this category when the AHU is of concern. There are three typical PID feedback control loops in a typical air-handling process as shown in Fig. 1, i.e., the supply air temperature controller, the return air flow rate controller and the static pressure air controller. Variables involved in these three control loops are considered in the qualitative model, including the supply air temperature (T_{sup}), supply air static pressure (P_{sup}), return air flow rate (M_{rtn}), supply air flow rate (M_{sup}), and control signals of the supply fan ($C_{fan,sup}$), return fan ($C_{fan,rtn}$) and the chiller water valve (C_{wat}). Since the supply air temperature and the return air humidity (h_{rtn}) are strongly coupled, the relationship between the supply air temperature and the return air humidity is also considered.

Fault patterns describing cause-effect relations between variables can be built as shown in Tables 2 and 3. These fault patterns describe sensor faults and their correspondent symptoms, which can be easily understood by checking the physical couplings among multiple variables in the air-handling processes. Each pattern is defined by the direction (negative or positive biases) of a faulty sensor and the change direction (increasing or decreasing magnitudes) of measurements of the affected variables.

Using faults of the supply air temperature sensor and the return air humidity sensor as examples, the establishment of fault patterns by expert-based multivariate decoupling is detailed as follows. Supposing that the supply air temperature sensor is faulty and its measurements have fixed positive biases, the control signal of the chilled water valve will be higher than it should be, resulting in a true supply temperature lower than the set point. Therefore, the ninth element of the residual vector is positive, and the eighth element is negative because the humidity in the supply air decreases due to the sensor fault. Similarly, if the supply air temperature is faulty and its measurement has a negative bias, the signs of the eighth and ninth elements of the residual vector are '+' and '−', respectively as shown in Table 2.

On the other hand, if the return air humidity senor is faulty and its measurements have fixed positive biases, the relationship between the return air humidity and the supply air temperature will be affected, and consequently the relationship between the return air humidity and the control signal of the chilled water will be affected as well. Therefore, if the return air humidity sensor is positively biased, the eighth element of the residual vector is positive and the fifth (corresponding to the supply air temperature) and the ninth element (corresponding to the control signal of the chilled water valve) of the residual vector are negative and positive, respectively. If the return air humidity sensor is negatively biased, conclusions can be made as shown in Table 2.

Similarly, according to the physical couplings among variables, signs of the residual elements under various sensor faults can be identified as shown in Tables 2 and 3.

Table 2
Fault patterns describing cause-effect relations in the heat balance model

Sensor fault (bias)	Affected variables								
	M_{fre} e_1	M_{sup} e_2	M_{rtn} e_3	T_{fre} e_4	T_{sup} e_5	T_{rtn} e_6	h_{fre} e_7	h_{rtn} e_8	$C_{val,wat}$ e_9
T_{sup} (+)	×	×	×	×	+	×	×	−	+
T_{sup} (−)	×	×	×	×	−	×	×	+	−
h_{rtn}(+)	×	×	×	×	−	×	×	+	+
h_{rtn}(−)	×	×	×	×	+	×	×	−	−

Table 3
Fault patterns describing cause-effect relations in the pressure-flow balance model

Sensor fault (bias)	Affected variables					
	M_{fre} e_1	M_{sup} e_2	M_{rtn} e_3	P_{sup} e_4	$C_{fan,sup}$ e_5	$C_{fan,rtn}$ e_6
M_{sup}(+)	×	+	+	−	−	+
M_{sup} (−)	×	−	−	+	+	−
M_{rtn}(+)	×	+	+	+	+	−
M_{rtn} (−)	×	−	−	−	−	+
P_{sup}(+)	×	−	−	+	−	−
P_{sup} (−)	×	+	+	−	+	+

'×' means uncertainty, '+' means positive sign and '−' means negative sign.

5. Tests and validation

Both simulation tests and tests using site data from an existing building were carried out to validate the PCA-based sensor FDD method for AHU [11,12]. In order to evaluate the performance of the isolation enhanced FDD method with expert-based multivariate decoupling, positive and negative biases were introduced to the same sensors in different tests, and the fault symptoms reflected by residual vectors are examined. Although it was found that the PCA models were sensitive to two typical component faults, i.e., cooling coil fouling and supply fan blade stuck in previous studies [11], they cannot be isolated from sensor faults easily. Using the expert-based isolation enhanced method, these component faults can be differentiated from sensor faults quantitatively. In order to test and validate the unique characteristics of sensor fault and component fault symptoms, the residual vectors of these two kinds of faults are presented and analyzed here. Results of a few tests are presented below to illustrate the performance of the joint isolation enhanced method.

5.1. Supply air temperature sensor faults

Two biases were introduced to the supply air temperature sensor in the air-handling process, one was the +1.0 K introduced at 11:40AM (which was failed to be isolated using the Q-contribution plot as shown in Fig. 4) and the other was −0.5 K introduced at 11:45AM. Fig. 6a shows that when the supply air temperature sensor was biased with +1.0 K, the residuals of the return air humidity and the chilled water valve control signal were negative and positive, respectively. Therefore, the signs of the residuals of the supply air temperature, return air humidity and chilled water valve control signal were '+', '−', '+', respectively. Comparing the fault symptoms with the fault patterns shown in Table 2, this fault could be correctly isolated. Under negative bias condition, signs of the residuals of the supply air temperature, return air humidity and chilled water valve control signal in the heat balance PCA model were '−', '+', '−', respectively as shown in Fig. 6b. Similarly, it could be correctly diagnosed by comparing the fault symptoms with the fault patterns shown in Table 2. Therefore, the fault isolation ability of the PCA-based FDD method is enhanced. It is also shown that the

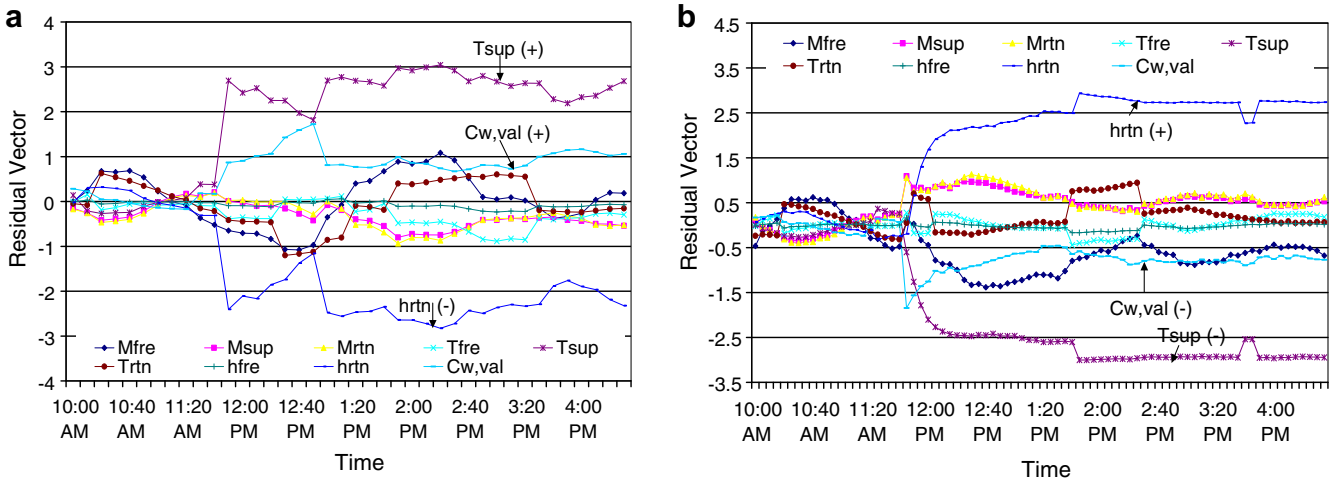

Fig. 6. Test results under the supply air temperature sensor faults – using the heat balance PCA model. (a) T_{sup} sensor biased with +1.0 K from 11:40 AM and (b) T_{sup} sensor biased with −0.5 K from 11:45 AM.

residuals of all variables fluctuated around zero, before the supply air temperature sensor faults occurred, and had much smaller magnitudes compared with those after the faults occurred.

5.2. Return air humidity sensor faults

Two fixed biases were introduced to the return air humidity sensor at different time. The results are shown in Fig. 7. Fig. 7a shows that under positive bias condition, the signs of the residuals of the supply air temperature, return air humidity and chilled water valve control signal were '−', '+', '+', respectively. Fig. 7b shows that, under negative bias condition, the residual of the supply air temperature was positive (+) and the cooled water control signal was negative (−). These two faults could be correctly isolated as well by comparing the fault symptoms and fault patterns.

5.3. Supply air flow rate sensor faults

Two fixed biases were introduced to the supply air flow rate sensor at different time. The validation results are shown in Fig. 8. Under the negative bias condition, the signs of the residuals of the return air flow rate, the static pressure and the control signals of the supply fan and return fan in the residual vectors of the pressure-flow balance PCA model were '−', '+', '+' and '−', respectively as shown in Fig. 8a. Under the positive bias condition, the signs were '+', '−', '−' and '+', respectively as shown in Fig. 8b. These two faults could be correctly isolated by comparing the fault symptoms with the fault patterns.

5.4. Return air flow rate sensor faults

Two fixed biases were introduced to the return air flow rate sensor in two tests, respectively. The results are shown in Fig. 9. Under the negative bias condition, the signs of the residuals of the supply air flow rate, the static pressure and the control signals of the supply fan and return fan in the residual vectors of the pressure-flow balance PCA model were '−', '−', '−' and '+', respectively as shown in Fig. 9a. Under the positive bias condition, the signs were '+', '+', '+' and '−', respectively as shown in Fig. 9b. It shows that these two faults could be correctly isolated using the isolation enhanced FDD method.

5.5. Supply air static pressure sensor faults

Two fixed biases were introduced to the supply air static pressure sensor at different time. Under both negative and positive bias

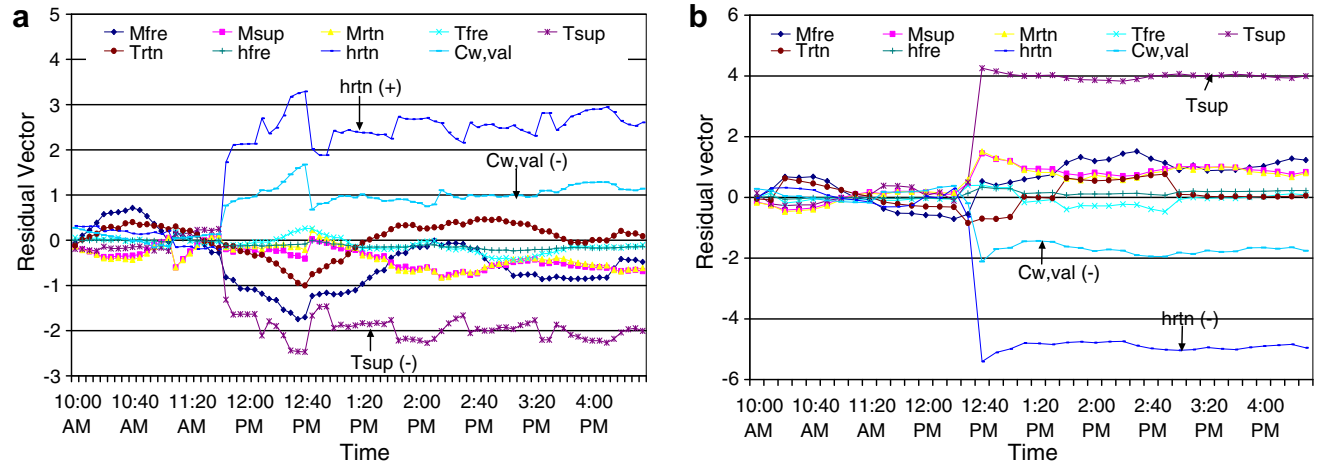

Fig. 7. Test results under the return air humidity sensor faults – using the heat balance PCA model. (a) h_{rtn} sensor biased with 5% from 11:45 AM and (b) h_{rtn} sensor biased with −10% from 12:40 AM.

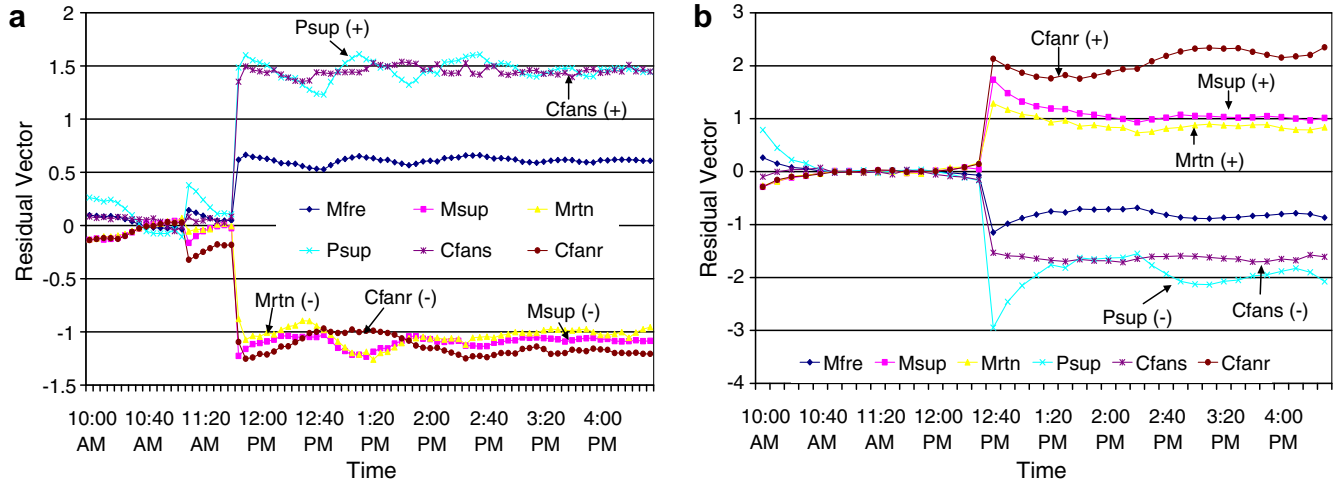

Fig. 8. Test results under the supply air flow rate sensor faults – using the pressure-flow balance PCA model. (a) M_{sup} sensor biased with −0.5 kg/s from 11:45 AM and (b) M_{sup} sensor biased with +1.0 kg/s from 12:40 AM.

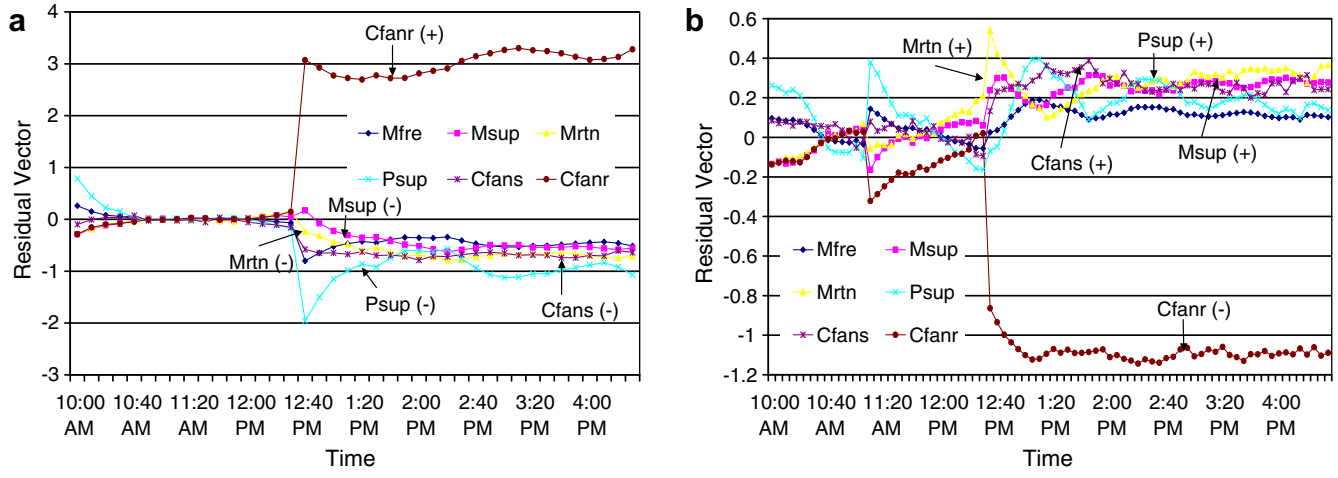

Fig. 9. Test results under the return air flow rate sensor faults – using the pressure-flow balance PCA model. (a) M_{rtn} sensor biased with −1.0 kg/s from 12:40 AM and (b) M_{rtn} sensor biased with +0.5 kg/s from 12:40 AM.

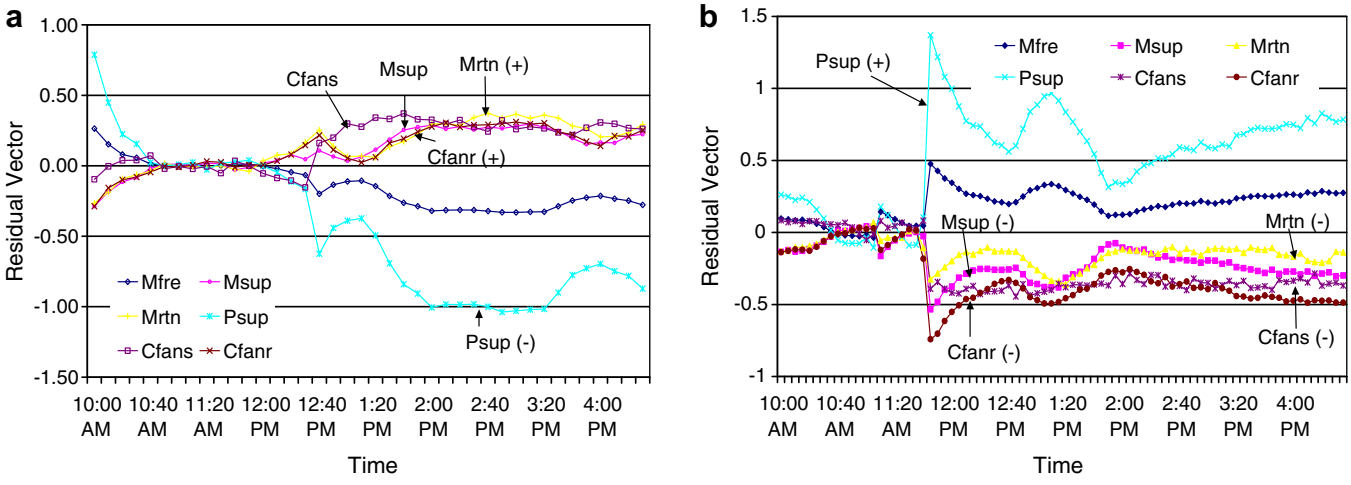

Fig. 10. Test results under the supply air static pressure sensor faults – using the pressure-flow balance PCA model. (a) P_{sup} sensor biased with −50 Pa from 12:40 AM and (b) P_{sup} sensor biased with +50 Pa from 11:45 AM.

conditions, the residuals of the control signals of the supply fan, the supply air flow rate, the return air flow rate and the control signal of the return fan had the same signs as shown in Fig. 10a and b, which were coincide with the fault patterns shown in Table 3. Therefore, these faults can be successfully isolated as well.

The test results validate that the expert-based multivariate decoupling approach enhances the sensor fault isolation ability of the PCA-based FDD method.

5.6. Cooling coil fouling

Due to fouling, the overall heat transfer efficiency of the cooling coil reduced gradually by 35% from 11:00AM to 2:00PM on the test day. The residual vector of the heat balance PCA model is shown in Fig. 11. With the development of the fouling severity, signs of the residuals of the supply air temperature and the return humidity sensor change, which causes fault symptoms inconsistent. However, a unique symptom of such a fault, which is different from those of sensor faults, is that the residuals of the control signals of the chilled water valve are the largest. Therefore, this kind of fault can be successfully isolated by combining the Q-contribution plot and symptoms of the residual vector of the heat balance PCA model.

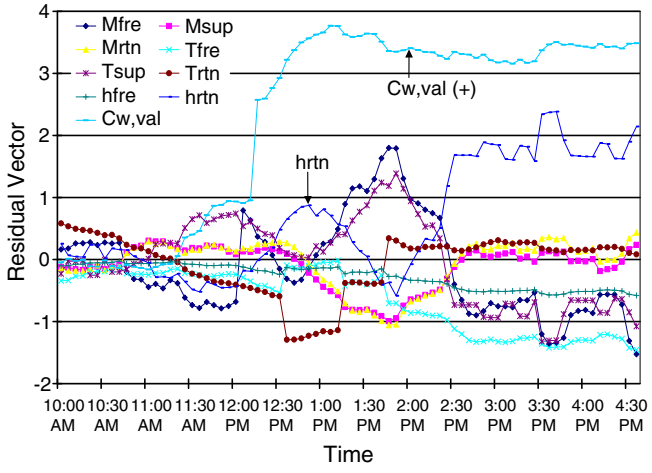

Fig. 11. Residual vectors of the heat balance PCA model when cooling coil fouling.

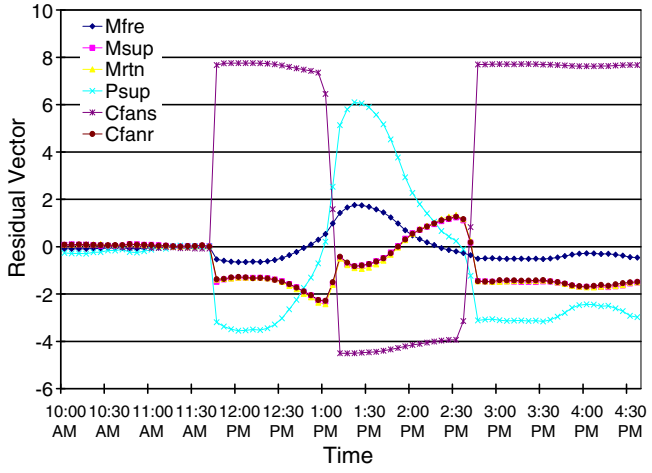

Fig. 12. Residual vectors of the pressure-flow balance PCA model when the supply fan blade was stuck at 15°.

5.7. Supply fan blade stuck

In this test, the supply fan blade was stuck at 15° from 11:40 AM. The pressure-flow balance PCA model is sensitive to such a fault. Fig. 12 shows the residual vectors of the pressure-flow balance PCA model. The supply fan control signals contribute most to the Q-statistics, and signs of the residuals of the control signals in the pressure-flow balance PCA model change from time to time. However, the control signals of the return fan and the supply fan give overwhelming contribution to the Q-statistic, which is unlike any sensor faults. Therefore, this fault can be isolated from sensor faults by the Q-contribution plot.

6. Conclusion

Although the PCA method has shown its powerful ability in detecting sensor faults in various engineering processes, its ability in diagnosing or isolating sensor faults is not satisfactory. The Q-contribution plot, which has been widely used to diagnose sensor faults, is not effective in isolating sensor faults whose effects may propagate to other parts in a process due to couplings. The expert-based multivariate decoupling approach developed in this study can supplement the Q-contribution plot, and provide much reliable fault isolation results while dealing with those sensor faults. By combining these two approaches together, physical knowledge about the process is planted into the pure data-driven PCA method. It makes the PCA method more effective and reliable while allowing the PCA model outputs more physically meaningful and understandable.

Fault patterns describing the fault directions (negative or positive biases) and the changing directions of affected variables (increasing or decreasing magnitudes) can be established by analyzing the couplings among multiple variables. In the improved PCA method, the changing directions of variables can be identified from the signs of corresponding elements in the residual vectors of PCA models. By comparing the fault patterns and fault symptoms reflected by the residual vectors, sensor faults could be correctly isolated. The method was applied to a typical VAV air conditioning system to detect and diagnose sensor faults. Test results show that the improved method is effective in detecting and isolating simple and complex sensor faults. The robustness of the sensor fault isolation approach is also improved because the fault pattern and fault symptom of a particular sensor fault are unique.

Acknowledgement

The research work presented in this paper was financially supported by Internal Competitive Research Grants in the Hong Kong Polytechnic University (G-YF85), Hong Kong SAR.

References

[1] J.J. Edward, A User's Guide to Principal Components, John Wiley, 1991.
[2] I.T. Jolliffe, Principal Component Analysis, Springer-Verlag, New York, 1986.
[3] R. Dunia, S.J. Qin, T.E. Edgar, T.J. McAvoy, Identification of faulty sensors using principal component analysis, AIChE Journal 104 (1) (1996) 2797–2812.
[4] R. Dunia, S.J. Qin, Joint diagnosis of process and sensor faults using principal component analysis, Control Engineering Practice 6 (1998) 457–469.
[5] E.L. Russell, L.H. Chiang, D.B. Richard, Fault detection in industrial processes using canonical variant analysis and dynamic principal component analysis, Chemometrics and Intelligent Laboratory Systems 21 (1) (2000) 81–93.
[6] J.H. Cho et al., Fault identification for process monitoring using kernel principal component analysis, Chemical Engineering Science 60 (1) (2005) 279–288.
[7] W.H. Li, H.H. Yue, S. Valle-Cervantes, S.J. Qin, Recursive PCA for adaptive process monitoring, Journal of Process Control 10 (2000) 471–486.
[8] F. Tsung, Statistical monitoring and diagnosis of automatic controlled processes using dynamic PCA, International Journal of Production Research 38 (3) (2000) 625–637.

[9] J. Lennox, C. Rosen, Adaptive multiscale principal components analysis for online monitoring of wastewater treatment, Water Science and Technology 45 (4–5) (2002) 227–235.
[10] N. Kaistha, B.R. Upadhyaya, Incipient fault detection and isolation of field devices in nuclear power systems using principal component analysis, Nuclear Technology 136 (2) (2001) 221–230.
[11] S.W. Wang, F. Xiao, Detection and diagnosis of AHU sensor faults using principal component analysis method, Energy and Buildings 36 (2004) 147–160.
[12] F. Xiao, S.W. Wang, J.P. Zhang, A diagnostic tool for online sensor health monitoring in air-conditioning systems, Automation in Construction 15 (2006) 489–503.
[13] S.W. Wang, Y.M. Chen, Sensor validation and reconstruction for building central chilling systems based on principal component analysis, Energy Conservation and Management 45 (2004) 673–695.
[14] J. Gertler, W.H. Li, Y.B. Huang, T. McAvoy, Isolation enhanced principal component analysis, AIChE Journal 45 (2) (1999) 323–334.
[15] H. Vedam, V. Venkatasubramanian, PCA-SDG based process monitoring and fault diagnosis, Control Engineering Practice 7 (1999) 903–917.
[16] S. Yoon, J.F. MacGregor, Fault diagnosis with multivariate statistical models part I: using steady state fault signatures, Journal of Process Control 11 (2001) 387–400.
[17] B.M. Wise, N.L. Ricker, Recent advances in multivariate statistical process control: improving robustness and sensitivity, in: K. Najim, J.P. Parbary (Eds.), IFAC International Symposium, ADCHEM'91, Toulouse, France, 1991, pp. 125–130.
[18] X.Q. Jin, Z.M. Du, Fault tolerant control of outdoor air and AHU supply air temperature in VAV air conditioning systems using PCA method, Applied Thermal Engineering 26 (2006) 1226–1237.
[19] Z.M. Du, X.Q. Jin, L.Z. Wu, Fault detection and diagnosis based on improved PCA with JAA method in VAV systems, Building and Environment 42 (2007) 3221–3232.
[20] S.W. Wang, Dynamic simulation of building VAV air-conditioning system and evaluation of EMCS Online Control Strategies, Building and Environment 34 (1999) 681–705.
[21] S.W. Wang, X.H. Xu, A robust control strategy for combining DCV control with economizer control, Energy Conversion and Management 43 (2002) 2569–2588.
[22] G. Avery, The instability of VAV systems, Heating/Piping/Air Conditioning 64 (1992) 47–50.
[23] J. Wang, Y. Wang, Performance improvement of VAV air conditioning system through feed forward compensation decoupling and genetic algorithm, Applied Thermal Engineering 28 (5–6) (2008) 566–574.
[24] R.G. Carlos, V.R. Miguel, Decoupled control of temperature and relative humidity using a variable-air-volume HVAC system and non-interacting control, in: IEEE Conference on Control Applications-Proceedings, 2001, pp. 1147–1151.
[25] H. Vedam, V. Venkatasubramanian, Signed diagraph based multiple fault diagnosis, Computer and Chemical Engineering 21 (S1) (1997) 655–660.
[26] F.L. Luo, C.Y. Wen, Multiple-page mapping artificial neural network algorithm used for constant tension control, Expert Systems with Applications 13 (4) (1997) 307–315.
[27] A.P. Oliva, W.C. Leite, Eigenstructure versus optimal control for decoupling, Control Engineering Practice 10 (10) (2002) 1059–1079.
[28] H.L. Shu, X.C. Guo, Decoupling control of multivariable time-varying systems based on PID neural network, in: Proceedings of 5th Asian Control Conference, vol. 1. 2004, pp. 682–685.
[29] F. Chatelin, Eigenvalues of Matrices, Wiley, New York, 1993.